

Static and Dynamic Stereochemistry of Hexaisopropylbenzene: A Gear-Meshed Hydrocarbon of Exceptional Rigidity

Jay Siegel,^{1a,b} Alberto Gutiérrez,^{1a} W. Bernd Schweizer,^{1c} Otto Ermer,^{1d} and Kurt Mislow*^{1a}

Contribution from the Department of Chemistry, Princeton University, Princeton, New Jersey 08544, the Organic Chemistry Laboratory, Swiss Federal Institute of Technology, ETH-Zentrum, CH-8092 Zürich, Switzerland, and the Abteilung für Chemie der Ruhr-Universität, Postfach 102148, D-463 Bochum, West Germany. Received June 11, 1985

Abstract: The crystal and molecular structure of hexaisopropylbenzene (**1**) has been analyzed by X-ray methods at 99 K: space group $P\bar{1}$, $a = 6.400$ (2) Å, $b = 9.943$ (3) Å, $c = 10.223$ (2) Å, $\alpha = 117.79$ (2)°, $\beta = 94.78$ (3)°, $\gamma = 105.58$ (3)°, $Z = 1$. The molecules closely approximate C_{6h} symmetry in the crystal. A crystallographic orientational disorder around the molecular sixfold axes was modeled with the help of simple structural and geometrical considerations. The molecular model thus derived accords well with the C_{6h} ground state calculated by the empirical force field (EFF) method. The relative energies of the nine conformers of **1** have been estimated by EFF calculations, and a one-to-one mapping of the conformers of **1** and hexaethylbenzene is developed. An improved approach for the synthesis of **1** has been devised, based on a novel method for obtaining the precursor, diisopropylacetylene. Cotrimerization of diisopropylacetylene with an elevenfold molar excess of diisopropylacetylene- d_{14} in the presence of $Hg[Co(CO)_4]_2$ gives a mixture of isotopomers in which **1- d_{28}** is the major isomer observable by 1H NMR spectroscopy. From the noncoalescence of the resonance-doubled signals of methyl and methine protons, a ΔG^\ddagger value of ≥ 22 kcal mol $^{-1}$ is estimated for the process of internal rotation in **1**. EFF calculations serve to rule out correlated rotation of the isopropyl groups. A reaction graph for stepwise rotation has been constructed and saddle points calculated for the individual transitions. These calculations indicate that the process of homomerization by rotation of all six isopropyl groups requires ca. 35 kcal mol $^{-1}$.

Geminal or vicinal isopropyl groups attached to a planar framework generally adopt bisected conformations in which the methine hydrogen of one group is tucked into the cleft formed by the two methyls of the neighboring group,² an example of static gearing.³ This gear effect is most strikingly exhibited by hexaisopropylbenzene (**1**):⁴ the six isopropyl groups form a tightly interlocking cyclic tongue-and-groove arrangement "by virtue of cooperative nonbonded repulsions".^{4a} Space-filling (CPK) models allow the construction of only this one conformation of **1**. This structure possesses C_{6h} symmetry, with all six isopropyl groups gear-meshed so that "each isopropyl group exactly interlock[s] with its neighbors on either side" and "all the groups are pointed in the same direction, clockwise or counterclockwise, around the perimeter of the ring".^{4a} The molecule thus adopts a "schaufelradähnliche Form".^{4d} This paper reports our investigation of the static and dynamic stereochemistry of this extraordinary compound.⁵

Synthesis of Hexaisopropylbenzene. Cyclotrimerization of diisopropylacetylene by $Co_2(CO)_8$ ^{4a,b} or $Hg[Co(CO)_4]_2$ ^{4d} is reported to afford **1** in 12%^{4a,b} or 3%^{4d} yield. The precursor, diisopropylacetylene, is obtained in 70% yield^{4b} by mercuric oxide oxidation of 2,5-dimethylhexane-3,4-dione bishydrazone,^{4b,6} itself obtained in only 3–4% yield by reaction sequences starting from 2,5-dimethylhex-3-yne-2,5-diol^{4a,b} or isobutyric acid.⁶ The overall yield of diisopropylacetylene is therefore only 2–3%,⁷ and that of

1 is less than 0.5%. While it was not clear whether the yield of the trimerization could be drastically improved, the astonishingly poor yields reported for diisopropylacetylene presented us with the need to develop a method capable of producing this compound conveniently and in reasonable yield.

After exploring a variety of standard approaches,⁸ we devised a new method based on a combination of procedures developed in a different context by Gribble et al.⁹ and by Nicholas et al.¹⁰ Commercially available 2,5-dimethylhex-3-yne-2,5-diol is reacted with $Co_2(CO)_8$; complexation occurs with concomitant loss of 2 equiv of carbon monoxide. A suspension of $NaBH_4$ in a methylene chloride solution of the acetylene complex is then treated with trifluoroacetic acid to yield the reduced acetylene-cobalt complex. Oxidation with ferric nitrate liberates diisopropylacetylene, which is purified by distillation. The yield of isolated product in this procedure is 70%. We were subsequently able to show that this facile method is generally useful for the synthesis of secondary alkylacetylenes.¹¹

When the neat acetylene is heated under reflux with 10 wt % of $Hg[Co(CO)_4]_2$, **1** is produced in ca. 30% yield. Accordingly, the overall yield of **1** is ca. 20%, an improvement by two orders of magnitude over previously reported⁴ procedures. We were thus enabled to carry out the experimental program described in this and a related paper.¹²

Molecular Structure of Hexaisopropylbenzene

Crystal Structure of Hexaisopropylbenzene. Early attempts to determine the crystal structure of **1** with room temperature diffraction data showed that although the crystals diffracted well, they were internally disordered.¹³ Data were then collected at 99 K and the structure of **1** was solved and refined assuming the space group $P\bar{1}$, with one molecule per unit cell centered on a special position. By treating these data by standard least-squares methods, two unique positions for each symmetry nonequivalent

(1) (a) Princeton University. (b) Swiss-American Exchange Scholar, 1983–1984. (c) Swiss Federal Institute of Technology. (d) Ruhr Universität.

(2) Berg, U.; Liljefors, T.; Roussel, C.; Sandström, J. *Acc. Chem. Res.* **1985**, *18*, 80 and references therein.

(3) Hounshell, W. D.; Iroff, L. D.; Iverson, D. J.; Wroczynski, R. J.; Mislow, K. *Isr. J. Chem.* **1980**, *20*, 65.

(4) (a) Arnett, E. M.; Bollinger, J. M. *J. Am. Chem. Soc.* **1964**, *86*, 4729.

(b) Bollinger, J. M. Ph.D. Dissertation, University of Pittsburgh, 1965. (c) Hopff, H. *Chimia* **1964**, *18*, 140. (d) Hopff, H.; Gati, A. *Helv. Chim. Acta* **1965**, *48*, 509.

(5) A portion of this work was reported in a preliminary communication: Siegel, J.; Mislow, K. *J. Am. Chem. Soc.* **1983**, *105*, 7763.

(6) Courtneidge, J. L.; Davies, A. G.; Luszyk, E.; Luszyk, J. *J. Chem. Soc., Perkin Trans. 2* **1984**, 155.

(7) Diisopropylacetylene has also been obtained in 7.5% yield by reaction of methylmagnesium bromide with 2,5-dichlorohex-3-yne (Levina, R. Ya.; Shabarov, Yu. S. *Dokl. Akad. Nauk SSSR* **1952**, *84*, 709; *Chem. Abstr.* **1953**, *47*, 3219d). However, the product is only 87% pure,^{4d} which may account in part for the very low yield in the subsequent cyclotrimerization.

(8) Iverson, D. J. Ph.D. Dissertation, Princeton University, 1981.

(9) Gribble, G. W.; Leese, R. M.; Evans, B. E. *Synthesis* **1977**, 172.

(10) Nicholas, K. M.; Pettit, R. *Tetrahedron Lett.* **1971**, 3475. Nicholas, K. M.; Pettit, R. *J. Organomet. Chem.* **1972**, *44*, C21. Connor, R. E.; Nicholas, K. M. *Ibid.* **1977**, *125*, C45.

(11) Nicholas, K. M.; Siegel, J. *J. Am. Chem. Soc.* **1985**, *107*, 4999.

(12) Singh, M. D. et al., to be published.

(13) Blount, J. F., private communication.

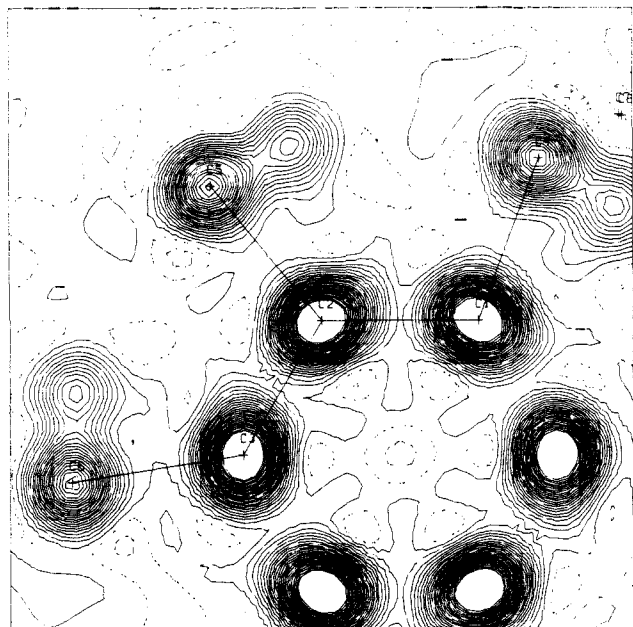


Figure 1. Electron density section of **1** through the least-squares plane of the benzene ring. Contour intervals are $0.5 e \text{ \AA}^{-3}$; zero contour dotted.

Table I. Final Fractional Crystal Coordinates for Hexaisopropylbenzene (**1**)^a

atom	x	y	z
C(1)	-0.4555 (2)	-0.4346 (2)	0.1589 (1)
C(2)	-0.3598 (2)	-0.3380 (1)	0.0987 (1)
C(3)	-0.4037 (2)	-0.4030 (1)	-0.0597 (2)
C(4)	-0.3826 (3)	-0.3365 (3)	0.3363 (2)
C(5)	-0.2028 (3)	-0.1570 (2)	0.1838 (2)
C(6)	-0.3160 (3)	-0.3212 (2)	-0.1520 (2)
C(7)	-0.5725 (3)	-0.3037 (2)	0.4130 (2)
C(8)	-0.2341 (3)	-0.3972 (2)	0.4048 (2)
C(9)	-0.3140 (2)	-0.0378 (2)	0.2767 (1)
C(10)	0.0297 (2)	-0.1262 (2)	0.2676 (1)
C(11)	-0.4065 (2)	-0.1874 (1)	-0.1339 (2)
C(12)	-0.0638 (2)	-0.2769 (2)	-0.1371 (2)
C(41)	-0.4586 (6)	-0.4195 (5)	0.3205 (3)
C(51)	-0.2192 (5)	-0.1712 (3)	0.2508 (4)
C(61)	-0.2604 (6)	-0.2514 (4)	-0.0695 (5)

^aStandard deviations in parentheses. For numbering of atoms, see scheme above, which corresponds to the stereoview in Figure 3. Average aromatic carbons $C_{ar}(av)$, C(1)–C(3); resolved methine carbons of major orientation C_t , C(4)–C(6); average methyl carbons $C_m(av)$, C(7)–C(12); resolved methine carbons of minor orientation C_t' , C(41)–C(61). Hydrogen parameters and anisotropic thermal motion coefficients are given in the supplementary material.

methine carbon (C_t) could be found, although only averaged positions could be obtained for each of the methyl (C_m) and aromatic (C_{ar}) positions. Splitting the population of the C_t 's between two sites per carbon (C_t and C_t') and refining on these populations resulted in a ca. 2:1 ratio of electron densities between the sites corresponding to one C_t (Figure 1, Table I). The observed disorder could be modeled by an arrangement of flipped rings in which the enantiotopic faces exchange places at various points in the packing, without order.¹⁴ However, if modeled in this manner, calculated X-ray molecular geometries of **1** (based

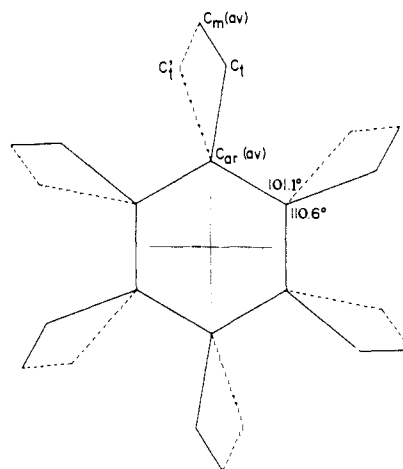


Figure 2. C_{6h} averaged geometry of **1** (view down the sixfold axis) based on the unresolved partially disordered structural model resulting from the crystallographic least-squares calculations. Full lines: major orientation. Dashed lines: minor orientation.

Table II. Comparison of Experimental and Calculated Structural Parameters of **1**^a

atoms ^b	av exptl (X-ray), partially disordered (major orientation) ^c	exptl (X-ray), disordered geometrically resolved ^c	calcd (EFF)
Bond Lengths			
$C_{ar}-C_{ar}$	1.406 (3)	1.416	1.419
$C_{ar}-C_t$	1.557 (0)	1.538	1.542
C_t-C_m	1.529 (2)	1.539	1.543
Bond Angles			
$C_{ar}-C_{ar}-C_{ar}$	120.0 (1)	120	120
$C_{ar}-C_{ar}-C_t^d$	129.4 (0)	120.4	121.1
$C_{ar}-C_{ar}-C_t^e$	110.6 (1)	119.6	118.9
$C_{ar}-C_t-C_m$	113.9 (1)	115.1	115.8
$C_m-C_t-C_m$	114.5 (2)	113.4	115.6
Torsion Angle			
$C_{ar}-C_{ar}-C_t-C_m$	67.0 (4)	67.4	70.1

^aBond lengths in angstroms, angles in degrees. ^b C_{ar} = aryl carbon, C_t = tertiary (methine) carbon, C_m = methyl carbon. ^cAveraged over C_{6h} symmetry, with average deviations in parentheses for the disordered model. ^dAngle anti with respect to methine hydrogen. ^eAngle syn with respect to methine hydrogen.

on the weighted average least-squares positions $C_{ar}(av)$ and $C_m(av)$, and on the resolved locations C_t and C_t' showed rather dramatic exocyclic angular distortions at $C_{ar}(av)$: for the major orientation, the averaged angles $C_{ar}(av)-C_{ar}(av)-C_t$ were found to be 129.4 and 110.6° (Figure 2, Table II), whereas empirical force field (EFF) calculations give deviations from the standard 120° value of only about 1° (Table II).¹⁵ For the minor orientation the angle distortions at $C_{ar}(av)$ are even more dramatic, $C_{ar}(av)-C_{ar}(av)-C_t' = 101.1$ and 138.9°.

Inspection of the electron density section through the benzene ring (Figure 1) and the thermal motion behavior of **1** (Figure 3) suggests, however, that the positions of the aromatic carbon atoms (C_{ar} and C_{ar}') differ appreciably. The $C_{ar}(av)$ electron density maxima are markedly elongated tangentially as are the corresponding anisotropic thermal motion ellipsoids. In addition, the thermal motion of the more peripheral (resolved) C_t and C_t' atoms is substantially smaller than that resulting from the least-squares

(14) An analogy can be drawn to an atactic polymer. Thus the 2:1 ratio is not a fixed number but a peculiarity of this crystal. It is quite conceivable that the ratio differs for individual crystals.

(15) Similar, small deviations are observed in tetraisopropylethylene, a statically geared molecule (C_{2h} symmetry) in which the methine hydrogens directionally eclipse the planar framework. See: Casalone, G.; Pilati, T.; Simonetta, M. *Tetrahedron Lett.* **1980**, 21, 2345.

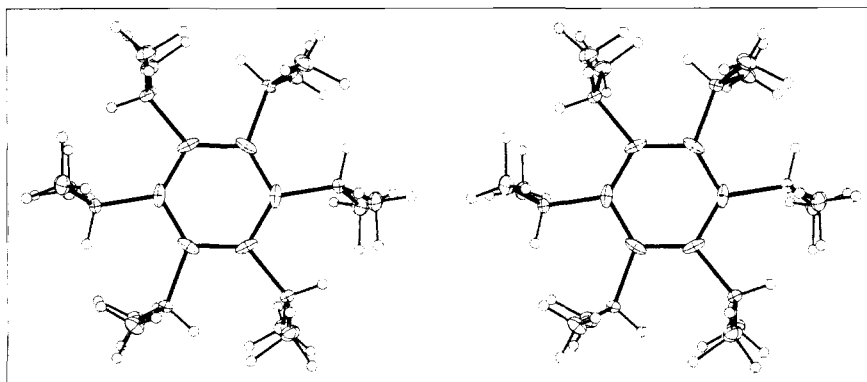


Figure 3. Stereoview of the major orientation of **1** down the approximate sixfold axis with thermal motion ellipsoids (50% probability). The drawing is based on resolved methine C_1 positions and average unresolved locations of the aryl and methyl carbon atoms, $C_{ar}(av)$ and $C_m(av)$, respectively, resulting from the crystallographic least-squares optimizations.

calculations for the more central (unresolved) $C_{ar}(av)$ atomic positions (Figure 3 and supplementary material), contrary to the expectation that **1** should act as a rigid body. Thus the pairwise averaged atomic positions of C_{ar} and C_m obtained from the standard crystallographic least-squares calculations are probably not reliable for deriving a sensible molecular geometry of **1**.

More sophisticated modeling can be effected under the following assumptions: (1) it is unlikely that the two orientations of **1** adopt drastically different internal geometries; (2) it is probable that the two flipped rings are rotated with respect to one another about an axis perpendicular to both rings. Under these assumptions, a geometric model was derived, as follows. First, the least-squares crystal coordinates were transformed to a Cartesian system with one axis perpendicular to the best plane through the positions of the aromatic and methine carbon atoms. Second, a set of C_{6h} averaged Cartesian coordinates was derived for $C_{ar}(av)$, C_1 , C_1' , and $C_m(av)$. Third, starting from the location of $C_{ar}(av)$, positions for C_{ar} and C_{ar}' were derived by opposite displacements in the ratio 2.075:1 (i.e., the population ratio of major and minor orientations; see Experimental Section) along an arc with radius $r = d(\text{origin}-C_{ar}(av))$, until corresponding angles $C_{ar}-C_{ar}-C_1$ and $C_{ar}'-C_{ar}'-C_1'$ became equal (Figure 4); the least-squares positions C_1 and C_1' were assumed completely resolved for this purpose. Fourth, resolved positions for C_m and C_m' were derived similarly by displacements applied to $C_m(av)$. Cartesian coordinates (in Å) for the geometrically resolved C_{6h} model are (symmetry-independent atoms only) the following: C_{ar} 0.1160, 1.4112, 0; C_1 0.2538, 2.9426, 0; C_m -0.2210, 3.6420, 1.2862.

Salient structural parameters of the partially resolved crystal structure (major orientation), the C_{6h} geometric model, and the force-field calculated ground state of **1** are collected in Table II. The tabulated set of experimental data confirms that C_{6h} symmetry is approximated within the standard deviations of the measured values.¹⁶

The present modeling scheme accords well with the ground-state structure of **1** calculated by the EFF method; most notably, both approaches yield standard values of ca. 120° for the $C_{ar}-C_{ar}-C_1$ angles. In principle, under the given assumptions concerning the disorder, the X-ray data could be modeled by the superposition of two of the EFF-calculated ground-state structures in lieu of the geometrically derived ones.

According to the geometric model, the distances between the crystal positions of corresponding carbon atoms of both orientations ($C_{ar}-C_{ar}'$, C_1-C_1' , and C_m-C_m') are 0.357, 0.769, and 0.115 Å. It is clear from these values that within the usual experimental X-ray conditions, crystallographic resolution of the disordered aromatic and methyl carbon atoms is out of the question.

(16) A similar situation is encountered in hexaethylbenzene, which has crystallographic $C_3(\bar{1})$ symmetry but whose molecular symmetry approximates $D_{3d}(3m)$ within the standard deviations of the measurements, despite the absence of threefold symmetry in the lattice (space group PI).¹⁷

(17) Iverson, D. J.; Hunter, G.; Blount, J. F.; Damewood, J. R., Jr.; Mislow, K. *J. Am. Chem. Soc.* **1981**, *103*, 6073.

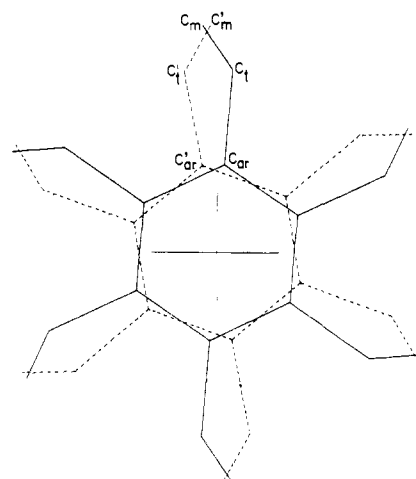


Figure 4. Geometrical resolution of the disorder in the crystal structure of **1**. The six-membered rings of the major and minor orientations (full and dashed lines, respectively) are rotated by 14.5° with respect to each other. The equivalent structures of both orientations represent averages over C_{6h} symmetry; the view is down the common sixfold axis. In contrast to the unresolved, partially disordered structure in Figure 2, corresponding angles $C_{ar}-C_{ar}-C_1$ and $C_{ar}'-C_{ar}'-C_1'$ in the geometric model are the same for both orientations (cf. Table II). Superposition of the major and minor orientations in the ratio of their population (2.075:1) yields a geometry identical with that of the structure in Figure 2.

Empirical Force Field Calculations. Molecular structures of hydrocarbons have been successfully modeled by EFF calculations.¹⁸ In the case of **1**, these calculations¹⁹ yielded a C_{6h} ground state, with structural parameters listed in Table II. The agreement between calculated and experimentally determined (geometrically resolved C_{6h} model; see above) values is satisfactory; the only somewhat larger discrepancy concerns the angle $C_m-C_1-C_m$ which is calculated ca. 2° larger than observed.

Additional EFF calculations¹⁹ showed that the nine possible conformational isomers of **1** in which all six isopropyl groups are

(18) Burkert, U.; Allinger, N. L. "Molecular Mechanics"; American Chemical Society: Washington, DC, 1982.

(19) Input geometries were based on standard bond lengths and bond angles. These structures were then optimized²⁰ by the program BIGSTRN-3²¹ using the MM2 force field.²² Final structures were characterized as minima by the absence of negative eigenvalues in the matrix of analytical second derivatives.

(20) Geometry optimizations were routinely begun with the variable-metric method and concluded with the full-matrix Newton-Raphson method; analytical second derivatives were used at both stages. The final convergence criteria for the Newton-Raphson stage were as follows: root-mean-square gradient less than 10^{-6} kcal mol⁻¹ Å⁻¹ and root-mean-square atom movement less than 10^{-6} Å.

(21) Nachbar, R. B., Jr.; Mislow, K., to be submitted to *QCPE*. A listing is available from the authors upon request.

(22) Allinger, N. L.; Yuh, Y. H. *QCPE* **1981**, *13*, 395. Two modifications for $C_{ar}-C_{ar}$ bonds were $l_0 = 1.3937$ Å and $k_s = 8.0667$ mdyne Å⁻¹. See also: Osawa, E.; Onuki, Y.; Mislow, K. *J. Am. Chem. Soc.* **1981**, *103*, 7475.

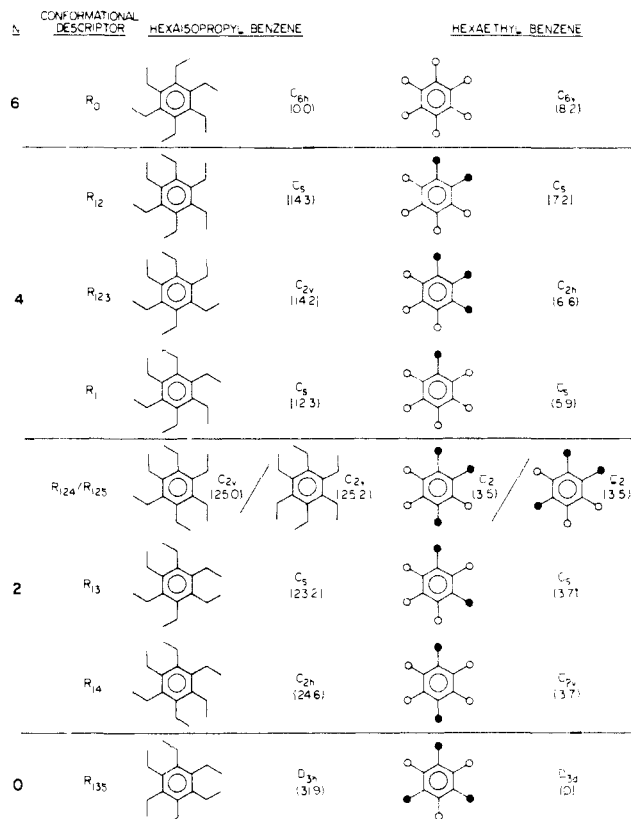


Figure 5. The nine conformational isomers of hexaisopropylbenzene (**1**) and hexaethylbenzene (**2**), their descriptors, highest symmetries, and relative EFF-calculated steric energies (in kcal mol⁻¹). Isomers of **1** are schematically represented by figures with lines projecting from the methine carbons that point in the direction of the methine hydrogens (methyl groups are not shown). Isomers of **2** are schematically represented by figures with filled and open circles that stand for methyl groups pointing toward and away from the observer.

constrained to adopt a bisected conformation correspond to nine distinct energy minima on the potential energy hypersurface, including the global minimum for the C_{6h} ground state. Schematic representations of these isomers, together with their calculated relative strain energies and their highest attainable symmetries, are shown in Figure 5.²³ Also shown in Figure 5 are the previously described¹⁷ conformers of hexaethylbenzene (**2**), together with their calculated relative strain energies²⁴ and their highest symmetries.²⁵ A one-to-one mapping of the two sets of isomeric structures is possible, based on the number and relative positions of alkyl groups turned by π from a standard structure of sixfold rotational symmetry in which all six alkyl groups point in the same direction. The mapping and the corresponding conformational descriptors²⁶ are displayed in Figure 5. It had previously been shown²⁷ that the conformers of **2** can be partitioned into four sets according to the number of syn interactions between ethyl groups

(23) Except for R_0 , all optimized structures have symmetries lower than those shown in Figure 5: C_1 (R_1 , R_{12} , R_{13}), C_2 (R_{14} , R_{123} , R_{124} , R_{125}), and D_3 (R_{135}). The desymmetrization results from deviations (up to 30°) of the $C_{ar}-C_{ar}-C_{i}-H$ torsion angle from 0°. Relative energies in Figure 5 refer to the actual minima of lower symmetry.

(24) These energies were calculated¹⁷ with use of another force field (Andose, J. D. et al. *QCPE* 1978, 10, 348) within the framework of the BIGSTRN-2 program (Iverson, D. J.; Mislow, K. *QCPE* 1981, 13, 410).

(25) As in the case of **1**, calculated structures of **2** are generally distorted to symmetries lower than the maximum attainable.¹⁷

(26) The descriptors are a modified version of the mnemonic labels employed for the conformers of hexakis(2-methylphenyl)benzene. See: Pepermans, H.; Gielen, M.; Hoogzand, C.; Willem, R. *Bull. Soc. Chim. Belg.* 1983, 92, 465. An arbitrary convention is adopted in which the numbering is clockwise from the top and in which the subscripts refer to the positions of the turned alkyl groups relative to a standard structure (R_0). The descriptors are not unique; thus $R_{125} \equiv R_{134} \equiv R_{146}$, $R_{123} \equiv R_{126}$, $R_{124} \equiv R_{136} \equiv R_{145}$, etc.

(27) Hunter, G.; Blount, J. F.; Damewood, J. R., Jr.; Iverson, D. J.; Mislow, K. *Organometallics* 1982, 1, 448.

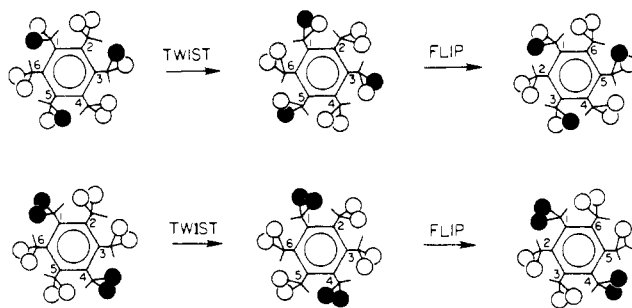


Figure 6. Labeled hexaisopropylbenzenes, with labeled and unlabeled methyl groups schematically represented by filled and open circles, respectively. In the twist process each isopropyl group is rotated by π , and in the flip process the molecule is rotated by π about the C(1)-C(4) axis. Top: C_3 symmetry. Bottom: C_{2h} symmetry.

in neighboring (ortho) positions whose methyls are located on the same side of the ring and that the calculated steric energies are qualitatively related to this number. It is therefore interesting to note that a similar relationship obtains for the conformers of **1**, which can be partitioned into four sets according to the number of gearing interactions between isopropyl groups in neighboring (ortho) positions. Figure 5 shows the grouping into sets, with N = number of ortho interactions. As in the case of **2**, the calculated steric energies are qualitatively related to N , except that the energy relationships are reversed: the fewer the gearing interactions, the higher the steric energy, whereas the fewer the syn interactions, the lower the energy. Thus **1** prefers to avoid neighboring isopropyl groups with methyl substituents oriented toward each other.

The relationship among conformers of **1** can thus be closely patterned on the previously described relationship among conformers of **2**,^{17,27} in particular, the four sets of isomers for **2** are paralleled by four sets for **1**. As will be noted in the next section, this parallelism can be extended into the dynamic domain.

Energetics and Mechanism of Internal Rotation in Hexaisopropylbenzene

The cyclic tongue-and-groove arrangement of isopropyl groups in **1** suggests that "rotation of the isopropyl groups is almost completely blocked",^{4a} i.e., that they are "nicht mehr rotationsfähig".^{4d} But just how immobilized is the gear-locked C_{6h} conformation, or, more precisely, what is the energy requirement for internal rotation in **1**? In the following sections we describe our attempts to provide an answer to this question.

Desymmetrization Strategies. Consider a process in which each of the six isopropyl groups in R_0 is twisted by π . Such a process (homomerization or automerization) results in a structure (R_{123456}) that is operationally indistinguishable from the one obtained by simply flipping the whole molecule by π . To observe the process of internal motion and to measure the attendant isopropyl group rotation barrier, the symmetry of **1** must therefore be lowered in some appropriate manner.

In one approach, which was successfully employed to determine the ethyl group rotation barrier in **2**,¹⁷ the two faces of the aromatic ring are rendered nonequivalent by complexation with $M(CO)_3$. In the case of **1**, such complexation would destroy plane and center of symmetry and lead to a chiral structure. Depending on its magnitude, the barrier to internal rotation could then be obtained from VT NMR (DNMR) measurements, by monitoring the site exchange of proximal and distal methyl groups resulting from rotation of the isopropyl side chains, or from conventional kinetics, by monitoring the racemization of the potentially optically active complex. However, **1** resists complexation,⁸ presumably because the ring is protected on both sides by bulky crowns of methyl groups.²⁸ It therefore became necessary to devise an alternative strategy.

(28) By the same token, steric crowding in such a π -complex, once formed, would be expected to change the alkyl group rotation barrier significantly because of an increase in ground-state energy.²⁹

(29) Iverson, D. J.; Mislow, K. *Organometallics* 1982, 1, 3.

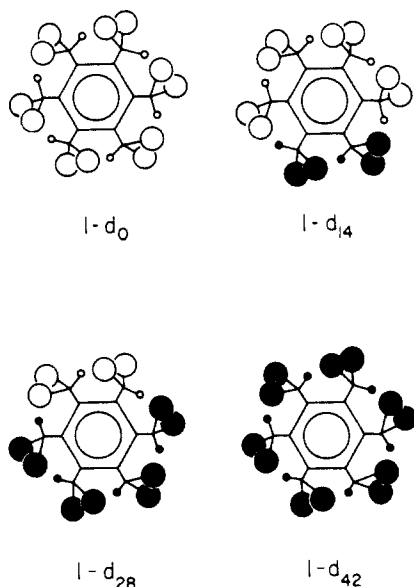


Figure 7. Four isotomers of **1**. Methyl groups and methine hydrogens are represented by large and small circles, respectively, and protium and deuterium atoms by open and filled circles, respectively.

One way to break the C_{6h} symmetry of **1** while minimizing the effect of chemical perturbation on the rotation barrier is to replace one or more methyls by CD_3 groups. In the design of molecules chemically modified in this manner, it must be kept in mind that structures capable of providing information on site-exchange processes, as monitored by DNMR, are limited to those whose symmetry does not contain C_3 as a subgroup.³⁰ Thus, the atoms in the initial structure on the top left of Figure 6 are located in an environment that is physically indistinguishable from the environment of the same atoms in the final structure on the top right, and the $R_0 \rightarrow R_{123456}$ process is therefore DNMR-invisible. Accordingly, DNMR experiments on labeled derivatives of **1** are restricted to structures which belong to C_{2h} or to one of its sub-symmetries (C_i , C_s , C_2 , and C_1). For example, the atoms at positions 2, 3, 5, and 6 in the initial structure on the bottom left of Figure 6 are located in an environment that is physically distinguishable from the environment of the same atoms in the final structure on the bottom right.

Molecular Rigidity of Hexaisopropylbenzene on the NMR Time Scale. We prepared a labeled derivative of the appropriate symmetry, with the positions of the labeled groups dictated by synthetic considerations. Cotrimerization of diisopropylacetylene with perdeuterated diisopropylacetylene in the presence of $Hg[Co(CO)_4]_2$ gave a mixture of the four isotomers shown in Figure 7, in which both cross-products, **1-d₁₄** and **1-d₂₈**, satisfy the criterion of C_{2h} subsymmetry (C_s). Of the two, **1-d₂₈** was chosen as the target molecule on the basis of the ready availability of 1H NMR and spectral simplicity.

Anticipating difficulties in the physical separation of the isotomers, we took advantage of our observation technique to create a spectroscopic window for the desired product by manipulation of the cross-product ratio in the trimerization. Disregarding possible isotope effects and starting with an equimolar ratio of the two acetylenes, the calculated percent product distribution is **1-d₀**:**1-d₁₄**:**1-d₂₈**:**1-d₄₂** = 1:3:3:1. But with an elevenfold molar excess of perdeuterated diisopropylacetylene, the distribution becomes 0.06:1.9:20.9:77.1.³¹ Under these conditions **1-d₀** and **1-d₄₂** are invisible, the former because it is present in trace

(30) The twist-flip process involves atom transpositions that are already implicit in the C_3 operation. For example, transpositions (26) and (35) in Figure 6 are contained in cyclic permutations (246) and (351), which may be expressed as products of overlapping transpositions (24)(26) and (35)(31) under the "replaced by" convention.

(31) According to this analysis, 84% of the available protons are incorporated in **1-d₂₈**, in fair agreement with a value of 89% calculated from relative MS intensities.

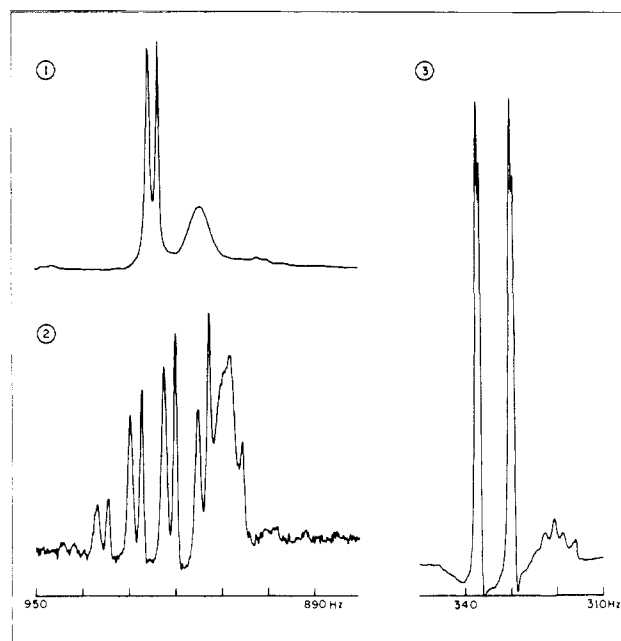


Figure 8. 250-MHz 1H NMR spectrum of **1-d₂₈** (also containing other isotomers) in $CDCl_3$ at room temperature. (1) Methyl-decoupled methine signals. The sharp doublet and the broad singlet arise from **1-d₂₈** and from molecules containing $CH(CD_3)_2$ groups, respectively. (2) Convolution difference, resolution-enhanced methine signals. The CH signal of **1-d₂₈** is now a doublet of septets ($J = 7.3$ Hz) with the outer lines barely visible (the scales of (1) and (2) are the same). (3) Convolution difference, resolution-enhanced methyl signals (doublet of doublets, $J = 7.3$ Hz); the high-field multiplet arises from CD_2H groups.

quantities and the latter because it contains no protons, while the cross-products **1-d₂₈** and **1-d₁₄** are present in a ratio of 11:1. In effect, **1-d₂₈** is thus isolated for observation.

In light of the spectroscopic evidence for internal congestion in **1**,³² there was reason to expect that an intrinsic steric isotope effect³³ would be manifested in the 1H NMR spectrum of **1-d₂₈**. Indeed it was found that the symmetry nonequivalence of the two $CH(CH_3)_2$ groups leads to resonance doubling in the methyl and methine regions ($\Delta\nu = 0.5$ and 2.4 Hz at 250 MHz, respectively) of the 1H NMR spectrum (Figure 8). The doubling remains apparent even at elevated temperatures (to $125^\circ C$, in decalin- d_{18}).³⁴ From these data, and using the Gutowsky-Holm approximation, a lower limit of $\Delta G^\ddagger = 22$ kcal mol⁻¹ was calculated³⁵ for the homomerization process in **1-d₂₈**. This value is also a lower limit for **1-d₀** since CD and CD_3 have smaller steric requirements than CH and CH_3 in conformational interconversion processes.³⁶

Empirical Force Field Calculations. In conjunction with the experimental studies described above, we employed EFF calculations in order to obtain an estimate of the homomerization barrier.^{19,37} First to be settled was the question of mechanism: do the isopropyl groups undergo correlated disrotation, i.e., are they dynamically geared,³ or does rotation proceed stepwise, one isopropyl group at a time? If all six groups were dynamically geared, R_0 would be converted to R_{123456} in a single step, via a

(32) Particularly significant is the sharp $C-H$ stretch at 3070 cm⁻¹ in the infrared spectrum.^{4a,d}

(33) Anet, F. A. L.; Dekmejian, A. H. *J. Am. Chem. Soc.* **1979**, *101*, 5449.

(34) We thank Mary W. Baum for technical assistance.

(35) Sandström, J. "Dynamic NMR Spectroscopy"; Academic Press: New York, 1982; p 96.

(36) Mislow, K.; Graeve, R.; Gordon, A. J.; Wahl, G. H., Jr. *J. Am. Chem. Soc.* **1964**, *86*, 1733.

(37) Stationary points were characterized as partial maxima by the number of negative eigenvalues in the force constant matrix; a single partial maximum (one negative eigenvalue) corresponds to a saddle point (transition state). Convergence criteria for saddle points were the same as for minima.²⁰ Transition structures were distorted along the negative and positive direction of the eigenvector associated with the negative eigenvalue and optimized by the variable-metric method; this assured that the saddle point connected the expected pair of minima.

transition state of D_{3d} symmetry in which the six isopropyl groups point alternately up and down around the benzene ring periphery. However, calculations showed that the D_{3d} conformation is a stationary point with three negative eigenvalues and a steric energy of 90.0 kcal mol⁻¹ relative to the C_{6h} ground state (R_0). One could still imagine the possibility of correlated rotation of just two neighboring isopropyl groups, leading from R_0 to R_{12} in a single step. However, this path was also ruled out by preliminary calculations which place the barrier at ca. 44 kcal mol⁻¹, while uncorrelated rotation requires a lower barrier, as discussed below. In short, the isopropyl groups in **1** undergo rotation one at a time, thus following the pattern of uncorrelated rotation observed or calculated for isopropyl groups in tetraisopropylethylene³⁸ and other statically geared systems.²

Homomerization by the stepwise mechanism requires passage through a structure in which three isopropyls have been turned, i.e., $R_0 \rightarrow R_1 \rightarrow R_{1x} \rightarrow R_{1xy}$. Since all R_{1xy} structures have at least one C_2 axis in the plane of the ring,²³ the three turned groups become equivalent to the three unturned ones and the mechanism of the last three steps, i.e. $R_{1xy} \rightarrow R_{123456}$, then follows from the principle of microscopic reversibility.

In determining the lowest-energy pathway for homomerization it is useful to construct a reaction graph for the system. In such a graph the vertices represent the conformers of **1** (corresponding to energy minima) and the connecting edges represent rearrangement steps and the associated transition structures (corresponding to saddle points). The relative energies of these stationary points need then be estimated, and from this information the preferred pathway can be deduced.

Consider any pair of conformers that can be interconverted by rotation of a single isopropyl group. Since the faces of the ring are enantiotopic, such neighboring conformers are interconverted through two enantiomeric transition structures. In the reaction graph these two enantiomeric pathways are represented by a single edge since the energies of the two saddle points must be exactly the same. Consider next the number of symmetry nonequivalent transition structures through which a given conformer is connected to all of its neighbors on the hypersurface; in the reaction graph this will be represented by the number of edges emanating from a given vertex, i.e., by the vertex degree. Because torsion of any one isopropyl group in either direction leads to enantiomeric pathways which are represented by a single edge, the vertex degree must be equal to the number of symmetry nonequivalent isopropyl groups in the corresponding conformer. Similar consideration had previously been advanced by one of us in conjunction with an analysis of conformational interconversions in tetraisopropylethylene.³⁸ However, whereas all the vertices in the tetraisopropylene graph are connected by single edges, three pairs of vertices in the reaction graph for **1** are connected by double edges, indicating that rotation of either of two symmetry nonequivalent isopropyl groups leads to the same conformer via two diastereomeric transition structures. Thus the two nonequivalent processes $R_1 \rightleftharpoons R_{12}$ and $R_1 \rightleftharpoons R_{16}$ both connect R_1 with R_{12} since $R_{12} \equiv R_{16}$. The same holds for $R_1 \rightleftharpoons R_{13}$ and $R_1 \rightleftharpoons R_{15}$, and for $R_{12} \rightleftharpoons R_{123}$ and $R_{12} \rightleftharpoons R_{126}$. The complete graph is depicted in Figure 9. Incidentally, we note that replacement of the conformers shown in Figure 9 by the corresponding conformers of **2** in Figure 5 yields a subgraph for the rearrangement of **2**.³⁹

The first step in the homomerization sequence must be $R_0 \rightarrow R_1$. The transition state for this process was calculated to lie 30.3 kcal mol⁻¹ above the ground state (R_0), an extraordinary barrier height when compared with most other sp^2 - sp^3 carbon-carbon single bond rotations.^{2,40} Six paths lead away from R_1 , including

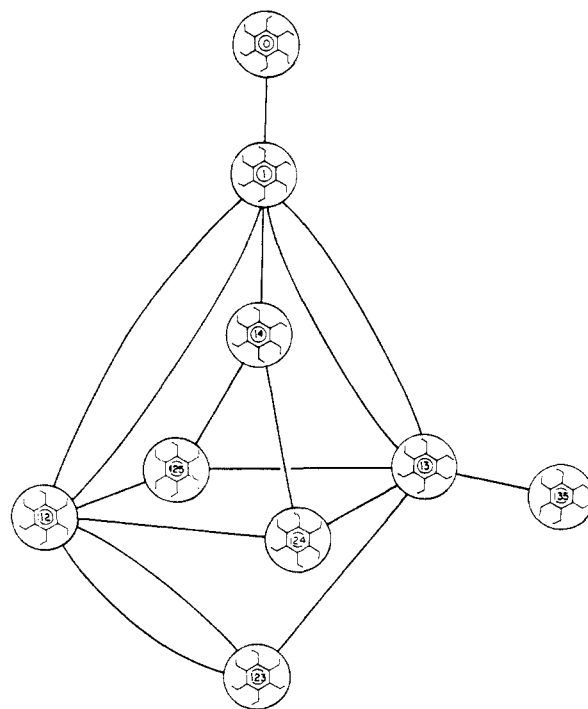


Figure 9. Graph showing symmetry nonequivalent pathways (edges) for the interconversion of the nine hexaisopropylbenzene conformers (vertices). Schematic representations as in Figure 5, with numerical descriptors centered in the rings.

the reverse of the first step ($R_1 \rightarrow R_0$). Calculated transition-state energies relative to R_0 are 35⁴¹ and 36.3 kcal mol⁻¹ for $R_1 \rightarrow R_{12}$ and $R_1 \rightarrow R_{16}$, respectively, 42⁴¹ and 38.2 kcal mol⁻¹ for $R_1 \rightarrow R_{13}$ and $R_1 \rightarrow R_{15}$, respectively, and 43.5 kcal mol⁻¹ for $R_1 \rightarrow R_{14}$. Accordingly, the energetically preferred second step leads from R_1 to R_{12} . Emanating from R_{12} are also six paths, two of which lead back to R_1 . For the two paths leading to R_{123} , calculated transition-state energies relative to R_0 are 38.3 and 34.7 kcal mol⁻¹ for $R_{12} \rightarrow R_{123}$ and $R_{12} \rightarrow R_{126}$, respectively; transition states were not calculated for the remaining two paths, which lead to intermediates of significantly higher energy (R_{124} and R_{125}). Accordingly, the energetically preferred third step leads from R_{12} to R_{126} . The remaining steps follow from the principle of microscopic reversibility, and the homomerization sequence is therefore established as $R_0 \rightarrow R_1 \rightarrow R_{12} \rightarrow R_{126} \rightarrow R_{1256} \rightarrow R_{123456}$, with an overall barrier of 35 kcal mol⁻¹. The results of our calculations are in qualitative agreement with our experimental observations on **1-d**₂₈ and leave little doubt that the isopropyl groups in **1** are rigidly locked in place on the laboratory or isolation time scale.⁴²

Experimental Section

Solution 250.13-MHz ¹H and 62.83-MHz ¹³C NMR spectra were recorded at ambient temperature on a Bruker WM-250 spectrometer. ¹H NMR spectra were also obtained on a JEOL FX-90Q spectrometer. Mass spectra were measured on an AEI MS-9 high-resolution mass spectrometer, with an ionizing voltage of 70 eV. Melting points were

(38) Ermer, O. *Angew. Chem., Int. Ed. Engl.* **1983**, *22*, 998.

(39) In the complete graph, the vertices representing the enantiomers R_{124} and R_{125} are each joined to R_{12} , R_{13} , and R_{14} by double rather than by single edges. This near-isomorphism is not apparent from the published graph for **2**¹⁷ because no double edges were drawn between $1e(R_1)$ - $1g(R_{12})$, $1e(R_1)$ - $1c(R_{13})$, and $1g(R_{12})$ - $1f(R_{123})$ and because the two enantiomers (R_{124} and R_{125}) were represented by a single vertex for **1d**.

(40) Sternhell, S. In "Dynamic Nuclear Magnetic Resonance Spectroscopy"; Jackman, L. M., Cotton, F. A., Ed. Academic Press: New York, 1975; Chapter 6. The current record holder, with $\Delta G^\ddagger = 39.1$ kcal mol⁻¹ at 200 °C and $\Delta H^\ddagger = 37.5$ kcal mol⁻¹, seems to be *o*-tolyl-1,1'-diadamantylcarbinol (Lomas, J. S.; Dubois, J.-E. *Tetrahedron* **1981**, *37*, 2273).

(41) The saddle point for this process did not converge, and the barrier energy was therefore calculated by the incremental group driving technique. The driven alkyl groups were rotated by 2° increments in the neighborhood of the saddle point. The constraints were released and the energy of the structure was minimized to assure that it converged to an adjacent minimum.

(42) On the other hand, rotation of the individual methyl groups is relatively free, with a calculated barrier of 1.6 kcal mol⁻¹. This bears out the conjecture by Arnett and Bollinger^{4a} that "there is no unusual restriction to normal rotation of the methyl groups around their own axes".

recorded on a Thomas Hoover melting point apparatus and are corrected.

Diisopropylacetylene. A 1-L round-bottom flask was charged under argon with 14.2 g (0.1 mol) of 2,5-dimethylhex-3-yne-2,5-diol (Farchan) in 300 mL of dichloromethane. To the solution was added 34.5 g (0.1 mol) of dicobalt octacarbonyl (Strem) and the mixture was allowed to stir for 6 h. The flask was then cooled in an ice-salt water bath and 11.2 g (0.3 mol) of sodium borohydride powder was suspended in the reaction mixture, followed by the dropwise addition of 100 mL of trifluoroacetic acid over a period of 30-60 min. After 3 h the reaction was quenched by decanting the solution away from the residual sodium borohydride onto ice. The organic phase was separated and washed again with water. Without drying, demetallation was effected by adding approximately 150 g of $\text{Fe}(\text{NO}_3)_3 \cdot 9\text{H}_2\text{O}$ to the well-stirred solution in an oversized beaker. The solution was then again decanted away from the residue which was washed with a small portion (50 mL) of dichloromethane. The organic phase was dried over sodium sulfate. Fractional distillation of the dichloromethane solution left a dark liquid from which 7.8 g (70% yield) of diisopropylacetylene (bp 102-105 °C (lit.^{4b} bp 104-106 °C)) was distilled. ^1H NMR (CDCl_3) δ 1.09 (d, 12 H, $J = 6.8$ Hz, $\text{CH}(\text{CH}_3)_2$), 2.48 (septet, 2 H, $J = 6.9$ Hz, $\text{CH}(\text{CH}_3)_2$) (lit.⁶ δ 1.05, 2.35 (CH_2Cl_2)). ^{13}C NMR (CDCl_3) δ 20.5 ($\text{CH}(\text{CH}_3)_2$), 23.5 ($\text{CH}(\text{CH}_3)_2$), 85.0 (acetylene carbon).

The above procedure was repeated with 2,5-dimethylhex-3-yne-2,5-diol- d_{14} ,⁴³ trifluoroacetic acid- d_1 , and NaBD_4 in place of the corresponding undeuterated reagents. The product, diisopropylacetylene- d_{14} , was characterized mass-spectrometrically and found to contain 97 atom % of deuterium.

Hexaisopropylbenzene. A 25-mL round-bottom flask was charged under argon with 5.0 g (45 mmol) of neat diisopropylacetylene and 0.5 g (1 mmol) of $\text{Hg}[\text{Co}(\text{CO})_4]_2$ ⁴⁴ as catalyst. The flask was fitted with a reflux condenser and the mixture was heated under reflux overnight. A solid formed on cooling. The reaction mixture was dissolved in chloroform and chromatographed on silica (60-240 mesh), using hexane as eluent. The desired product was obtained as a white, crystalline solid, 1.6 g (31% yield), mp 285-287 °C (lit.^{4a} mp 286 °C; lit.^{4d} mp 286-286.5 °C). ^1H NMR (CDCl_3) δ 1.22 (d, 36 H, $J = 7.2$ Hz, $\text{CH}(\text{CH}_3)_2$), 3.68 (septet, 6 H, $J = 7.2$ Hz, $\text{CH}(\text{CH}_3)_2$) (lit.^{4a,b} δ 1.27, 3.61 (CS_2)). ^{13}C NMR (CDCl_3) δ 22.9 (C_m), 27.6 (C_i), 144.7 (C_{ar}).

The above procedure was repeated with a mixture of diisopropylacetylene (0.5 g, 5 mmol) and diisopropylacetylene- d_{14} (7.0 g, 56 mmol),

with 0.5 g of $\text{Hg}[\text{Co}(\text{CO})_4]_2$. After chromatography on silica gel the isotopomer mixture was obtained as a white solid (2.3 g, 31%), mp 287-288 °C, after recrystallization from pentane-ethanol.

Mass spectral peak heights were averaged over ten runs at 20 eV. Corrections were made for natural isotopic distribution in a hydrocarbon of formula $\text{C}_{24}\text{H}_{42}$. The adjusted data were then fit to Biemann's formula⁴⁵ and a percent distribution of isotopomers was obtained: d_{42} 82.6; d_{28} 15.8; d_{14} 1.3; $d_0 \sim 0$.

X-ray Crystallography. Crystals of **1** were obtained from a mixture of pentane and ethanol (3:1) by slow evaporation at -20 °C. A crystal of approximately $0.20 \times 0.25 \times 0.40$ mm³ was chosen for the X-ray measurements. Crystal data: $\text{C}_{24}\text{H}_{42}$, $M_r = 330.34$ g mol⁻¹; triclinic (space group $P\bar{1}$ assumed throughout); $a = 6.400$ (2) Å, $b = 9.943$ (3) Å, $c = 10.223$ (2) Å, $\alpha = 117.79$ (2)°, $\beta = 94.78$ (3)°, $\gamma = 105.58$ (3)°, $V = 536.7$ Å³; $d_x = 1.022$ g cm⁻³, $Z = 1$. X-ray intensities were collected at 99 K on a four-circle diffractometer (CAD4) equipped with a nitrogen-flow cooling device applying Mo $K\alpha$ radiation ($\lambda = 0.71069$ Å). A total of 3737 independent reflections were recorded with $\theta_{\text{Mo}} < 30^\circ$ of which 2699 with $I > 3\sigma(I)$ were considered significant. The structure was solved by direct methods with MULTAN.⁴⁶ The carbon atoms were refined anisotropically, the hydrogens isotropically, by full-matrix least-squares with use of the 1964 significant reflections with $\sin \theta/\lambda > 0.45$ Å⁻¹. Common population coefficients p and p' were refined for the methine carbons C_i and C'_i of the major and minor orientations, respectively, with the constraint $p + p' = 1$; the final value of p was 0.6748 (200). R and R_w factors after the refinement were 0.045 and 0.045, respectively.

Acknowledgments. We thank the National Science Foundation (CHE-8009670) for support of this work and Daniel Iverson and Robert Pascal for helpful discussions.

Registry No. **1**, 800-12-4; 2,5-dimethylhex-3-yne-2,5-diol, 142-30-3; diisopropylacetylene, 927-99-1.

Supplementary Material Available: Final anisotropic thermal parameters for carbon atoms, atomic coordinates of hydrogen atoms, and isotropic temperature factors, with standard deviations, for **1** (3 pages). Ordering information is given on any current masthead page.

(43) This compound was prepared by reaction of acetylene and ethylmagnesium bromide, followed by addition of acetone- d_6 to the Grignard reagent and hydrolysis of the adduct with D_2O . Recrystallization from hexane gave a product (mp 89-91 °C) which was found by MS to contain 99 atom% of deuterium.

(44) Dighe, S. V.; Orchin, M. *Inorg. Chem.* **1962**, *1*, 965.

(45) Biemann, K. "Mass Spectrometry"; McGraw-Hill: New York, 1962.

(46) Main, P. "MULTAN 80; a System of Computer Programs for the Automatic Solution of Crystal Structures from X-ray Diffraction Data"; Department of Physics, University of York: York, England, 1980.

Study of ^{13}C - ^{13}C NMR Coupling Constants in α -Cyanodiarylmethyl and 1,1-Diaryl-2-butynyl Cations¹

V. V. Krishnamurthy, G. K. Surya Prakash, Pradeep S. Iyer, and George A. Olah*

Contribution from Donald P. and Katherine B. Loker Hydrocarbon Research Institute and Department of Chemistry, University of Southern California, University Park, Los Angeles, California 90089-1661. Received July 1, 1985

Abstract: One-bond ^{13}C - ^{13}C NMR coupling constants in α -cyanodiarylmethyl and 1,1-diaryl-2-butynyl cations were measured and compared to those in related neutral model compounds. The substituent effects on chemical shifts (SCS) and coupling constants (SCC) are discussed in light of charge delocalization into the neighboring cyano group or triple bond through contributing mesomeric nitrenium and allenyl cation structures. While $J_{\text{C}-\text{C}_\alpha}$ reflects the change in the bond order between C_i and C_α with respect to the nature of the substituent on the aryl ring, $J_{\text{C}_\alpha-\text{C}_\beta}$ is relatively insensitive to such changes.

It is well-known that one-bond ^{13}C - ^{13}C coupling constants, J_{CC} , can be correlated to the percents character of the orbitals making up the bond.²⁻⁴ Recently we reported⁵ one-bond ^{13}C - ^{13}C coupling

constants in a series of acetophenones, benzaldehydes, and their O-protonated carboxonium ions using the INADEQUATE⁶ pulse

(1) Stable Carbocation. 266. For Part 265, see: de Meijere, A.; Schallner, O.; Goltz, P.; Weber, W.; Schleyer, P. v. R.; Prakash, G. K. S.; Olah, G. A. *J. Org. Chem.* **1985**, *50*, 5255.

(2) Graham, D. M.; Holloway, C. E. *Can. J. Chem.* **1963**, *41*, 2114.

(3) Frei, K.; Bernstein, H. J. *J. Chem. Phys.* **1963**, *38*, 1216.

(4) Lynden-Bell, R. M.; Sheppard, N. A. *Proc. R. Soc. London, Ser. A* **1962**, *269*, 385.